A Hybrid Efficient Iterative ACA-PO and Chebyshev Approximation Technique for Fast Radiation Analysis Over a Broad Frequency Band

Junjun Wu

Chinese Flight Test Establishment
Xi'an City 710089, Shaanxi Province, China
wu18792802634@outlook.com

Abstract – In this paper, a novel approach integrated efficient iterative adaptive cross approximation-physical optics (EI-ACA-PO) and Chebyshev approximation technique (CAT) is proposed to efficiently calculate the broadband solution of antenna placed on electrically large platforms. The adaptive cross-approximation (ACA) method is employed to compress the self-impedance matrix of the Method of Moments (MoM) region, and the interaction matrices between the MoM and physical optics (PO) regions. By introducing CAT technology, the iterative hybrid method is capable of efficiently calculating the wideband results. First, the outer surface is divided into two regions. Then, the integral equation is solved by the EI-ACA-PO method to obtain the induced current at the Chebyshev nodes. Afterwards, the current in a desired frequency band is represented by the Chebyshev series. To improve accuracy, the Chebyshev series is matched with the Maehly approximation. The current at any frequency point in the bandwidth can be calculated. Finally, the broadband electromagnetic radiation characteristics can be obtained.

Index Terms – Adaptive cross-approximation (ACA), carrier antenna analysis, Chebyshev approximation technique (CAT), hybrid method, iterative technology.

I. INTRODUCTION

In recent years, broadband radiation analysis of integrated antenna-platform systems has become increasingly critical for modern wireless systems. Early radiation analysis of integrated antenna-platform systems primarily relied on full-wave numerical methods such as the Method of Moments (MoM) [1]. These methods achieve electromagnetic modeling by precisely discretizing both platform and antenna structures, but they face exponential growth in unknowns when dealing with electrically large platforms, leading to prohibitive computational costs. To address this, high-frequency approximation methods such as physical optics (PO) [2] were widely adopted. PO simplifies calculations by neglecting the coupling between field triangles, making it suitable for rapid estimation of radiation characteristics at high frequencies. However, it struggles to accurately model complex phenomena arising from antenna coupling.

The hybrid method of MoM and PO is effective for modeling the electromagnetic problems of antennas around platforms [3–9]. In hybrid analysis, the entire structure is divided into MoM-regions and PO-regions. It is assumed that the currents in the PO-region are radiated and excited by the currents in the MoM-region. Then, the PO contributions can either be coupled into the MoM impedance matrix on the left-hand side of the equation, or represented in the equation as additional excitations, with an iterative approach used to drive the system to a steady state. Meanwhile, algorithms like adaptive cross approximation (ACA) [10] and multilevel fast multipole algorithm (MLFMA) [11] emerged, significantly improving the efficiency of full-wave methods. They are also integrated into hybrid methods, such as MLFMA combined with PO (MLFMA-PO) [12], ACA combined with PO (ACA-PO) [13] and adaptive integral method (AIM) combined with PO (AIM-PO) [14].

Nevertheless, confronted with the wideband challenges, these techniques still require independent matrix factorization for each frequency point, which leads to enormous time consumption. The process of repetitive solution of the matrix equations can be bypassed when employing the Chebyshev approximation technique (CAT) [15] and asymptotic waveform evaluation (AWE) [16]. Compared with AWE, CAT is widely used due to its better convergence and easier integration with other methods without adding additional memory.

In this paper, a hybrid efficient iterative adaptive cross approximation-physical optics (EI-ACA-PO)-CAT method is presented to achieve efficient wideband radiation analysis of antenna around electrically large platforms. In the proposed method, the whole PEC system can be divided into two regions: ACA-region and PO-region. the initial current coefficients in the ACA-region at the Chebyshev nodes can be independently

Submitted On: May 19, 2025
Accepted On: July 01, 2025

https://doi.org/10.13052/2026.ACES.J.410204

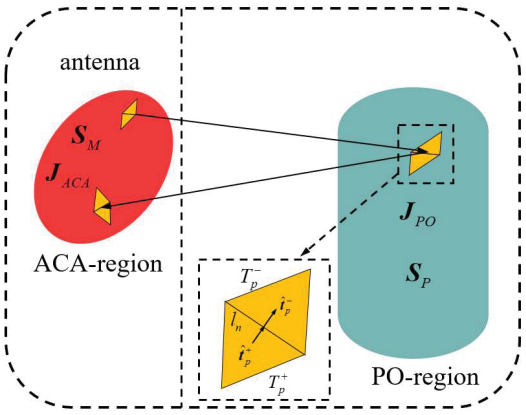

Fig. 1. EI-ACA-PO model of the perfect electric conductor (PEC) system.

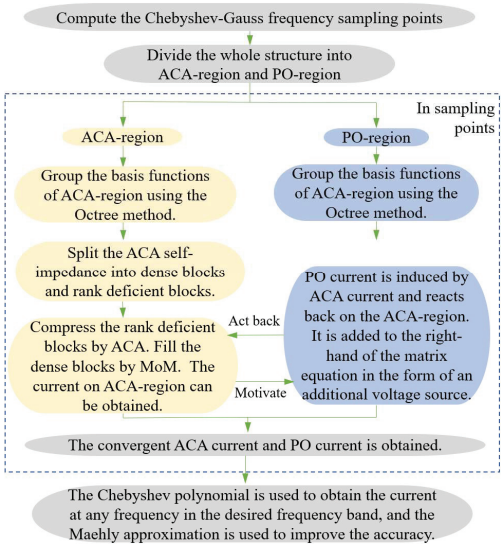

Fig. 2. Flow chart of the EI-ACA-PO-CAT method.

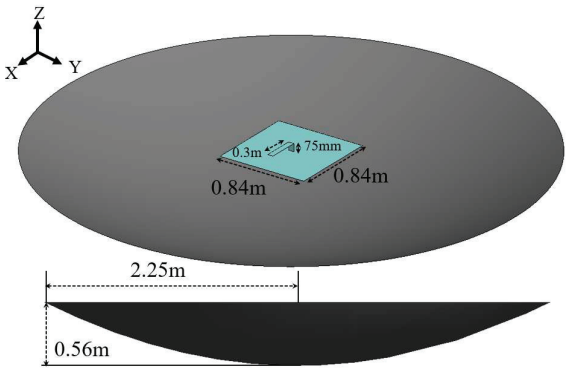

Fig. 3. Geometry of the inverted-L antenna placed above a paraboloid.

calculated by ACA. An iterative process is implemented to make the system become stable and obtain the current coefficients that have converged in two regions at Chebyshev nodes. CAT is employed to expand the current coefficients at any frequency point over the desired frequency band. Finally, to achieve a better accuracy, the Chebyshev series is transformed into a rational function by applying the Maehly approximation. Numerical examples show that the EI-ACA-PO-CAT can significantly improve calculation efficiency without loss of accuracy.

II. EI-ACA-PO-CAT FORMULATION

Consider an antenna mounted onto a perfectly conducting carrier. In the hybrid EI-ACA-PO-CAT analysis, the whole system is divided into two parts, namely the ACA-region and the PO-region. The surface currents in the ACA-region and the PO-region are denoted $\boldsymbol{J}_{ACA}$ and $\boldsymbol{J}_{PO}$, respectively, as depicted in Fig. 1. The desired frequency band and the corresponding wave number band are represented by $[f_a, f_b]$ and $[k_a, k_b]$, respectively. Generally, the scattered fields $(\boldsymbol{E}^s, \boldsymbol{H}^s)$ induced by the current $\boldsymbol{J}$ can be expressed as

$$\boldsymbol{E}^s = \boldsymbol{L}^E \boldsymbol{J}, \tag{1}$$

$$\boldsymbol{H}^s = \boldsymbol{L}^H \boldsymbol{J}, \tag{2}$$

where

$$\boldsymbol{L}^E \boldsymbol{J} = -jk\eta \int_S \left[\boldsymbol{J} G(\boldsymbol{r}, \boldsymbol{r}') + \frac{1}{k^2} \nabla \nabla' \boldsymbol{J} G(\boldsymbol{r}, \boldsymbol{r}') \right] ds', \tag{3}$$

$$\boldsymbol{L}^H \boldsymbol{J} = \nabla \times \int_S \boldsymbol{J} G(\boldsymbol{r}, \boldsymbol{r}') ds', \tag{4}$$

where $k = \omega\sqrt{\mu_0 \varepsilon_0}$ is the wavenumber, $\eta = (\varepsilon_0/\mu_0)^{1/2}$ is the wave impedance, $G(\boldsymbol{r}, \boldsymbol{r}') = e^{-jk|\boldsymbol{r}-\boldsymbol{r}'|}/(4\pi|\boldsymbol{r}-\boldsymbol{r}'|)$ denotes the Green's function of free space. $\boldsymbol{r}$ and $\boldsymbol{r}'$ are the observation and source points.

In the Chebyshev approximation approach, first, we need to compute the $Q+1$ Chebyshev-Gauss frequency sampling points $\tilde{k}_q$ that are the roots of the Chebyshev polynomial $T_{Q+1}(x)$ by

$$\tilde{k}_q = \cos\left[\frac{\pi(2q+1)}{2(n+1)}\right], \quad q = 0, 1, 2, \ldots, Q, \tag{5}$$

where Q is the truncated order of the Chebyshev series. These Chebyshev-Gauss sampling points need to be mapped from the interval $[-1, 1]$ to the desired band $[k_a, k_b]$ by

$$k_q = \frac{1}{2}[\tilde{k}_q(k_b - k_a) + (k_b + k_a)]. \tag{6}$$

After obtaining the frequency sampling points k_q, we calculate the initial current coefficients in the

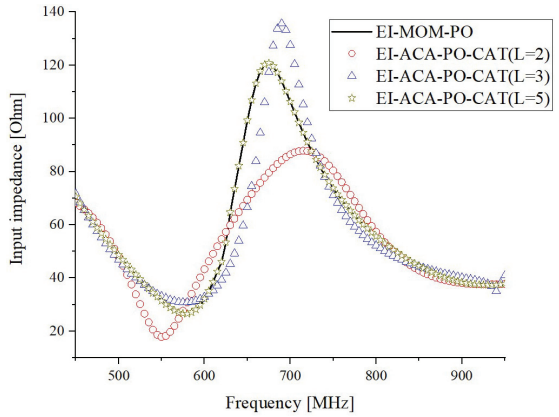

Fig. 4. Input impedance frequency response of an inverted-L antenna placed above a PEC plane by using three different orders of EI-ACA-PO-CAT.

Table 1: CPU time and memory requirement of different methods for the inverted-L antenna placed above a paraboloid

Method	Number of Unknowns		Sweep Points	Memory (MB)	Total CPU Time (s)	RMSE
	ACA	PO				
EI-MoM-PO	1512	10142	101	1396.5	45961	\
EI-ACA-PO-CAT (L=2)				1414.4	582	13.11
EI-ACA-PO-CAT (L=3)				1443.4	663	9.72
EI-ACA-PO-CAT (L=5)				1444.8	1314	0.1

ACA-region at each k_q using pure ACA method. Assume that there are M basis functions situated in the ACA-region and P basis functions existing within the PO-region. The total number of basis functions for the EM system is defined as $N = M + P$. Using the PEC boundary condition and Galerkin testing procedure, the matrix equation at the sampling points can be set up as

$$\boldsymbol{Z}^{ACA}(k_q)\boldsymbol{I}^{0,ACA}(k_q) = \boldsymbol{V}(k_q), \tag{7}$$

where the superscript 0 of $\boldsymbol{I}^{0,ACA}(k_q)$ denotes the number of iterations. The basis functions of the ACA-region are grouped by the octree method, and the self-impedance matrix $\boldsymbol{Z}^{ACA}$ is now a block structure with rank deficient off-diagonal blocks. By using the standard ACA to decompose the off-diagonal blocks, the MVM can be expressed as

$$\begin{aligned}
\boldsymbol{Z}^{ACA}\boldsymbol{I}^{0,ACA} &= (\boldsymbol{Z}^{ACA}_{dia} + \boldsymbol{Z}^{ACA}_{od})\boldsymbol{I}^{0,ACA} \\
&= \begin{pmatrix} \boldsymbol{Z}^{ACA}_{dia(1,1)} & \cdots & \boldsymbol{Z}^{ACA}_{od(1,n)} \\ \vdots & \ddots & \vdots \\ \boldsymbol{Z}^{ACA}_{od(n,1)} & \cdots & \boldsymbol{Z}^{ACA}_{dia(n,n)} \end{pmatrix} \boldsymbol{I}^{0,ACA} \\
&= \sum_{i=1}^{N_{dia}} (\boldsymbol{Z}^{ACA}_{dia(i_x,i_y)} \cdot \boldsymbol{I}^{0,ACA}_{(i_x,i_y)}) \\
&\quad + \sum_{i=1}^{N_{od}} (\boldsymbol{Z}^{ACA}_{od(i_x,i_y)} \cdot \boldsymbol{I}^{0,ACA}_{(i_x,i_y)}) \\
&= \sum_{i=1}^{N_{dia}} (\boldsymbol{Z}^{ACA}_{dia(i_x,i_y)} \cdot \boldsymbol{I}^{0,ACA}_{(i_x,i_y)}) \\
&\quad + \sum_{i=1}^{N_{od}} ((\boldsymbol{L}^{ACA}_{m_i \times r_i} \cdot \boldsymbol{R}^{ACA}_{r_i \times n_i}) \cdot \boldsymbol{I}^{0,ACA}_{(i_x,i_y)}),
\end{aligned} \tag{8}$$

where the subscripts *dia* and *od* represent the diagonal blocks and the off-diagonal blocks, respectively. N_{dia} and N_{od} are the total number of $\boldsymbol{Z}^{ACA}_{dia}$ and $\boldsymbol{Z}^{ACA}_{od}$. (i_x, i_y) is the serial number of ith block. $\boldsymbol{I}^{0,ACA}_{(i_x,i_y)}$ is the corresponding part in vector $\boldsymbol{I}^{0,ACA}$. $\boldsymbol{L}^{ACA}_{m_i \times r_i}$ and $\boldsymbol{R}^{ACA}_{r_i \times n_i}$ are dense rectangular matrices obtained by compression of $\boldsymbol{Z}^{ACA}_{dia(i_x,i_y)}$. m_i and n_i denote the dimension of $\boldsymbol{Z}^{ACA}_{dia(i_x,i_y)}$. r_i is the effective rank.

Let us now consider the effect of the PO-region. For radiation, we suppose that the impressed fields just exist at the feeding point of the antenna. Consequently, the current in the PO-region is only induced by the ACA current solved by (7). The basis functions in the PO-region are also grouped through the octree method, resulting in interaction matrices with block structures. Blocks formed by sufficiently separated basis function groups in both ACA- and PO-regions are defined as far-field matrix blocks. These blocks possess low-rank characteristics and can be accelerated via ACA:

$$\begin{aligned}
\boldsymbol{I}^{i,PO} &= \boldsymbol{\tau}^{PO\text{-}ACA}\boldsymbol{I}^{i-1,ACA} \\
&= (\boldsymbol{\tau}^{PO\text{-}ACA}_{\text{far}} + \boldsymbol{\tau}^{PO\text{-}ACA}_{\text{near}})\boldsymbol{I}^{i-1,ACA} \\
&= \left(\sum_{a=1}^{N_{\text{far}}} \boldsymbol{L}^{PO\text{-}ACA}_{N^a_{PO} \times r^a_{PO\text{-}ACA}} \boldsymbol{R}^{PO\text{-}ACA}_{rPO\text{-}ACA^a \times N^a_{ACA}} \right) \boldsymbol{I}^{i-1,ACA} \\
&\quad + \tau^{PO\text{-}ACA}_{\text{near}} \boldsymbol{I}^{i-1,ACA}, \quad i = 1, 2, \ldots, Iter,
\end{aligned} \tag{9}$$

where i stands for the ith iterative process and *Iter* is the total number of iterations. The induced current in the PO-region will inversely affect the ACA-region. It is added to the right-hand side of (7) in the form of additional exciting voltages, expressed as

$$\boldsymbol{V}^i = \boldsymbol{V} + \Delta\boldsymbol{V}^i, \tag{10}$$

$$\begin{aligned}
\Delta\boldsymbol{V}^i &= -\boldsymbol{Z}^{ACA\text{-}PO}\boldsymbol{I}^{i,PO} \\
&= (\boldsymbol{Z}^{\text{far}}_{ACA\text{-}PO} + \boldsymbol{Z}^{\text{near}}_{ACA\text{-}PO}) \cdot \boldsymbol{I}^{i,PO}
\end{aligned}$$

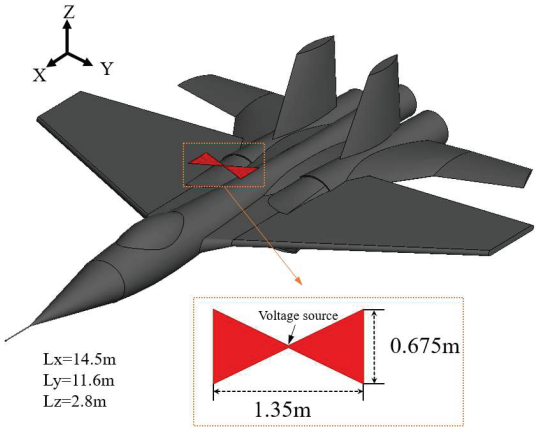

Fig. 5. Geometry of a trapezoidal dipole antenna placed above the aircraft.

$$= \left[\left(\sum_{j=1}^{N_{\text{far}}} \boldsymbol{L}^{\text{ACA-PO}}_{N^j_{ACA} \times r^j_{ACA\text{-}PO}} \boldsymbol{R}^{\text{ACA-PO}}_{r^j_{ACA\text{-}PO} \times N^j_{ACA}} \right) + \boldsymbol{Z}^{\text{near}}_{ACA\text{-}PO} \right] \cdot \boldsymbol{I}^{i,PO}, \tag{11}$$

where $r^j_{ACA\text{-}PO}$ and $r^a_{PO\text{-}ACA}$ are the effective ranks of jth matrix block of $\boldsymbol{Z}^{\text{far}}_{ACA\text{-}PO}$ and ath block of $\boldsymbol{\tau}^{\text{far}}_{PO\text{-}ACA}$. $r^j_{ACA\text{-}PO} < \min(N^j_{ACA}, N^j_{PO})$, $r^a_{PO\text{-}ACA} < \min(N^a_{ACA}, N^a_{PO})$, $\boldsymbol{L}^{PO\text{-}ACA}_{N^a_{\text{PO}} \times r^a_{PO\text{-}ACA}}$ and $\boldsymbol{R}^{PO\text{-}ACA}_{r^a_{PO\text{-}ACA} \times N^a_{ACA}}$, $\boldsymbol{L}^{ACA\text{-}PO}_{N^j_{ACA} \times r^j_{ACA\text{-}PO}}$ and $\boldsymbol{R}^{ACA\text{-}PO}_{r^j_{ACA\text{-}PO} \times N^j_{ACA}}$ represent two dense rectangular matrices obtained by compressing the far-field matrix blocks, respectively.

Then we apply the iterative process from (10) to (11) until the current in the ACA-region stabilizes. The error ε_i is used to evaluate whether the ACA current is stable, expressed as

$$\varepsilon_i = \frac{\|\boldsymbol{I}^{i,ACA} - \boldsymbol{I}^{i-1,ACA}\|}{\|\boldsymbol{I}^{i-1,ACA}\|}, \tag{12}$$

where $\|\cdot\|$ is the 2-norm.

Once the currents $\boldsymbol{I}^{ACA}(k_q)$ and $\boldsymbol{I}^{PO}(k_q)$ at the sampling frequencies are obtained, any surface current $\boldsymbol{I}^{ACA/PO}(k)$ within the desired frequency band $[k_a, k_b]$ can be given by Chebyshev series as

$$I_n(k) = \sum_{q=0}^{Q} c_{n,q} T_q(k_q) - \frac{c_{n,0}}{2}, \tag{13}$$

where the Chebyshev polynomial satisfies the recursion relation as

$$\begin{cases} T_0(x) = 1 \\ T_1(x) = x \\ T_{n+1}(x) = 2xT_n(x) - T_{n-1}(x) \end{cases}, \quad x \in [-1,1], \quad n = 1,2,\ldots,\infty, \tag{14}$$

where $\boldsymbol{m}_q$ are the expanding coefficients.

$$c_{n,q} = \frac{2}{Q} \sum_{q=1}^{Q+1} I_n(k_q) T_q(\tilde{k}_q), \quad q = 1,2,\ldots,Q. \tag{15}$$

Chebyshev series typically employ the Maehly approximation [15] for rational functions. By integrating the Maehly approximation with Equation (13), the components of $\boldsymbol{I}(k)$ are reformulated as

$$\begin{aligned} I_n(k) &\cong \sum_{q=0}^{Q} c_{n,q} T_q(k_q) - \frac{c_{n,0}}{2} \\ &= \frac{\sum_{i=0}^{L} a_{n,i} T_i(\tilde{k}_q)}{1 + \sum_{j=1}^{M} b_{n,j} T_j(\tilde{k}_q)} \\ &\Rightarrow \sum_{i=0}^{L} a_{n,i} T_i(\tilde{k}_q) \\ &= \left(\sum_{p=0}^{\infty} c_{n,p} T_p(\tilde{k}_q) - \frac{c_0}{2} \right) \\ &\quad \times \sum_{j=0}^{M} b_{n,j} b_{n,j} T_j(\tilde{k}_q) \\ &= \sum_{j=0}^{M} b_{n,j} \sum_{p=0}^{\infty} c_{n,p} T_p(\tilde{k}_q) T_j(\tilde{k}_q) \\ &\quad - \frac{1}{2} \sum_{j=0}^{M} b_{n,j} c_{n,0} T_j(\tilde{k}_q), \end{aligned} \tag{16}$$

where $Q = L + 2M$. According to the identity property $T_i(x)T_j(x) = \frac{1}{2}[T_{i+j}(x) + T_{|i-j|}(x)]$ Equation (16) can be simplified as

$$\begin{aligned} &\sum_{i=0}^{L} a_{n,i} T_i(k_q) \\ &= \left(\frac{1}{2} c_{n0} b_{n0} + \frac{1}{2} \sum_{j=1}^{M} b_{n,j} c_{n,j} \right) T_0(k_q) \\ &\quad + \sum_{l=1}^{\infty} \left[b_{n,0} c_{n,l} \right. \\ &\quad \left. + \frac{1}{2} \sum_{j=1}^{M} b_{n,j} (c_{n,j+l} + c_{n,|l-j|}) \right] T_l(k_q). \end{aligned} \tag{17}$$

By matching the two sides, the coefficients in the numerator and the denominator can be obtained by

$$\begin{cases} a_{n,0} = \frac{1}{2} \sum_{j=1}^{M} b_{n,j} c_{n,j} + \frac{1}{2} b_{n,0} c_{n,0} \\ a_{n,i} = \sum_{j=1}^{M} \frac{1}{2} b_{n,j} (c_{n,|i-j|} + c_{n,j+i}) + b_{n,0} c_{n,i} \\ \quad i = 1,2,\ldots,Q \end{cases}$$

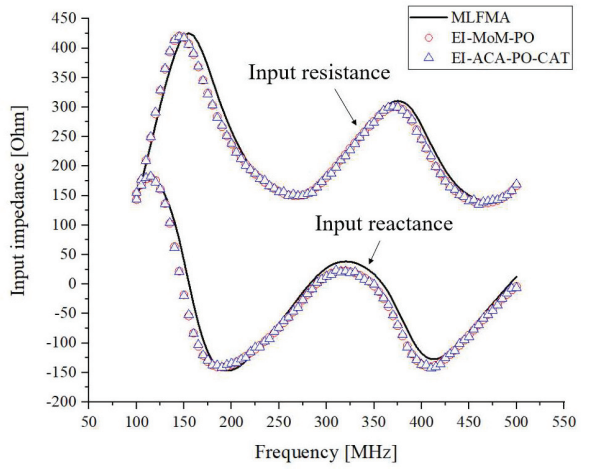

(a)

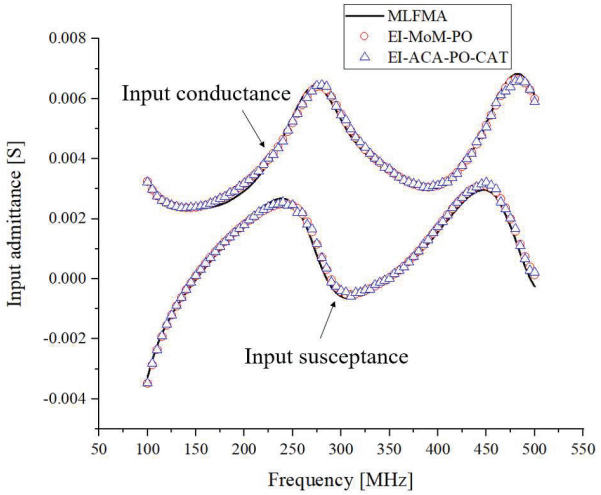

(b)

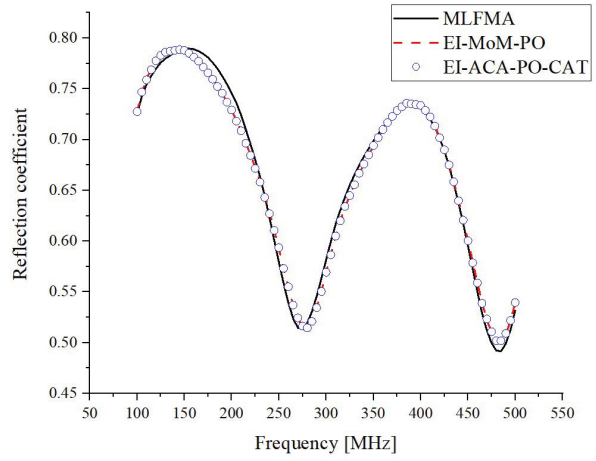

(c)

Fig. 6. Wideband results obtained from EI-ACA-PO-CAT compared with MLFMA and EI-MoM-PO methods: (a) input impedance, (b) input admittance, (c) reflection coefficient.

Table 2: CPU time and memory requirement of different methods for a trapezoidal dipole antenna placed above the aircraft

Method	Number of Unknowns		Sweep Points	Memory (MB)	Total CPU Time (s)
	ACA	PO			
MLFMA	108904	\	81	35026	43888
EI-MoM-PO	1269	25959		3106	58401
EI-ACA-PO-CAT(L=7)				3127	12256

$$\begin{bmatrix} c_{n,L}+c_{n,L+2} & \cdots & c_{n,L-M+1}+c_{n,L+M+1} \\ c_{n,L+1}+c_{n,L+3} & \cdots & c_{n,L-M+2}+c_{n,L+M+1} \\ \cdots & \cdots & \cdots \\ c_{n,L+M-1}+c_{n,L+M+1} & \cdots & c_{n,L}+c_{n,L+2M} \end{bmatrix} \times \begin{bmatrix} b_{n,1} \\ b_{n,2} \\ \cdots \\ b_{n,M} \end{bmatrix} = -2 \begin{bmatrix} c_{n,L+1} \\ c_{n,L+2} \\ \cdots \\ c_{n,L+M} \end{bmatrix}. \tag{18}$$

Finally, the current coefficients at any point within the desired frequency band can be obtained. For ease of understanding, a flowchart of the EI-ACA-PO-CAT method is shown in Fig. 2.

III. NUMERICAL RESULTS

In this section, two simple examples are demonstrated to show the accuracy and efficiency of the proposed EI-ACA-PO-CAT method for fast analysis of antennas on platforms over a broad frequency band. The error tolerance of the iteration between ACA- and PO-regions is selected as 0.003. All results are produced on a 64-bit PC with 3.67 GHz of CPU and 48 GB of RAM.

A. Inverted-L antenna placed above a paraboloid

The first example is an inverted-L antenna placed above a paraboloid. The dimensions of the structure are depicted in Fig. 3. The inverted-L antenna is mounted on the center of a PEC rectangular plane. The length and width are both 0.84 m. An ideal slot voltage source is set at the connection edge between the antenna and the plane. The paraboloid has an aperture radius of 2.25 m and a depth of 0.56 m. In hybrid analysis, the antenna and the plane are selected as the ACA-region, and the paraboloid is the PO-region. The desired frequency band ranges from 450 MHz to 950 MHz. The ACA- and PO-regions are discretized into 1042 and 6821 triangles, leading to 1512 and 10142 basis functions, respectively.

Figure 4 shows the input impedance obtained from EI-ACA-PO-CAT with three different ($L = M = 2, 3, 5$)

order results and the EI-MoM-PO method. It is observed that there are significant errors in the second and third order of EI-ACA-PO-CAT but the result of the fifth order just agrees with EI-MoM-PO solution. In order to better represent the differences, the root mean square error (RMSE) is defined as follows

$$\mathrm{RMSE} = \sqrt{\frac{1}{Num}\sum_{i=1}^{Num}(y_i - y_i^{EI\text{-}MOM\text{-}PO})^2}, \qquad (19)$$

where *Num* is total number of the results. The superscript of y means the method. Table 1 displays the memory, total CPU time and RMSE compared EI-ACA-PO-CAT method with EI-MoM-PO. Although the proposed EI-ACA-PO-CAT costs a bit more memory, it can significantly reduce the CPU time compared to direct calculation with the EI-MoM-PO.

B. Trapezoidal dipole antenna placed above the aircraft

In the second example, we consider a trapezoidal dipole antenna placed above the aircraft. The dimensions of the structure are depicted in Fig. 5. The trapezoidal dipole antenna is defined as the ACA-region, and the aircraft is defined as the PO-region. An ideal slot voltage source is set at the center of the trapezoidal dipole antenna. The desired frequency band ranges from 100 MHz to 500 MHz with 5 MHz spacing. For the full-wave method, the whole system is discretized into 72622 triangles, leading to 108904 basis functions. For the hybrid analysis, the ACA- and PO-regions are discretized into 754 and 21724 triangles, leading to 1269 and 25959 basis functions, respectively.

Figures 6 (a–c) show the input impedance, the input admittance and the reflection coefficient obtained by EI-ACA-PO-CAT ($L = M = 7$) compared with the MLFMA and the EI-MoM-PO method. It is observed that the results of the EI-ACA-PO-CAT method are in good agreement with the results of the direct sweep calculation of the other two methods. Table 2 shows the comparison of memory consumption and computing time from different methods. The EI-ACA-PO-CAT method achieves a significant reduction in computing time without taking up too much memory.

IV. CONCLUSION

This paper proposes a novel approach integrating efficient iterative adaptive cross approximation-physical optics (EI-ACA-PO) and Chebyshev approximation technique (CAT) to efficiently calculate broadband solutions for antennas mounted on electrically large platforms. The outer surface is divided into ACA- and PO-regions, where the ACA method compresses the self-impedance matrix of the ACA-region and interaction matrices between ACA- and PO-regions. The iterative technology further reduces computational complexity. CAT is introduced to solve the surface integral equation at Chebyshev nodes using EI-ACA-PO to obtain induced currents, which are used by Chebyshev series and Maehly approximation to calculate currents at any frequency point in the desired bandwidth, finally deriving the broadband electromagnetic radiation characteristics. This method effectively addresses the challenge of efficient broadband computation for antennas mounted on the electrically large platform by combining matrix compressing and frequency-interpolation approximation, ensuring both computational efficiency and accuracy.

REFERENCES

[1] S. Rao, D. Wilton, and A. Glisson, "Electromagnetic scattering by surfaces of arbitrary shape," *IEEE Trans. Antennas Propag.*, vol. 30, no. 3, pp. 409–418, May 1982.

[2] U. Jakobus and F. M. Landstorfer, "Improved PO-MM hybrid formulation for scattering from three-dimensional perfectly conducting bodies of arbitrary shape," *IEEE Trans. Antennas Propag.*, vol. 43, no. 2, pp. 162–169, Feb. 1995.

[3] U. Jakobus and F. I. C. Meyer, "A hybrid physical optics/method of moments numerical technique: Theory, investigation and application," in *Proc. IEEE AFRICON*, Stellenbosch, South Africa, vol. 1, pp. 282–287, Sep. 1996.

[4] J. Ma, S.-X. Gong, X. Wang, Y. Liu, and Y.-X. Xu, "Efficient wideband analysis of antennas around a conducting platform using MoM-PO hybrid method and asymptotic waveform evaluation technique," *IEEE Trans. Antennas Propag.*, vol. 60, no. 12, pp. 6048–6052, Dec. 2012.

[5] W.-J. Zhao, J. L.-W. Li, and L. Hu, "Efficient current-based hybrid analysis of wire antennas mounted on a large realistic aircraft," *IEEE Trans. Antennas Propag.*, vol. 58, no. 8, pp. 2666–2672, Aug. 2010.

[6] C. S. Kim and Y. Rahmat-Samii, "Low profile antenna study using the physical optics hybrid method (POHM)," in *Proc. Antennas Propag. Soc. Symp. Dig.*, London, ON, Canada, vol. 3, pp. 1350–1353, June 1991.

[7] R. E. Hodges and Y. Rahmat-Samii, "An iterative current-based hybrid method for complex structures," *IEEE Trans. Antennas Propag.*, vol. 45, no. 2, pp. 265–276, Feb. 1997.

[8] Z.-L. Liu and C.-F. Wang, "Efficient iterative method of moments: Physical optics hybrid technique for electrically large objects," *IEEE Trans. Antennas Propag.*, vol. 60, no. 7, pp. 3520–3525, July 2012.

[9] Z.-L. Liu, X. Wang, and C.-F. Wang, "Installed performance modeling of complex antenna array mounted on extremely large-scale platform using fast MoM-PO hybrid framework," *IEEE Trans. Antennas Propag.*, vol. 62, no. 7, pp. 3852–3858, July 2014.

[10] K. Zhao, M. N. Vouvakis, and J.-F. Lee, "The adaptive cross approximation algorithm for accelerated method of moments computations of EMC problems," *IEEE Trans. Electromagn. Compat.*, vol. 47, no. 4, pp. 763–773, Nov. 2005.

[11] C. B. Wu, L. Guan, P. F. Gu, and R. S. Chen, "Application of parallel CM-MLFMA method to the analysis of array structures," *IEEE Trans. Antennas Propag.*, vol. 69, no. 9, pp. 6116–6121, Sep. 2021.

[12] Y. Zhang and H. Lin, "MLFMA-PO hybrid technique for efficient analysis of electrically large structures," *IEEE Antennas Wireless Propag. Lett.*, vol. 13, pp. 1676–1679, 2014.

[13] Z. Xu, X. Wang, H. Zhang, L. Zhao, C. Liu, and Y. Liu, "A hybrid method of ACA-PO for efficient analysis of antenna array mounted on electrically large platforms," *IEEE Trans. Antennas Propag.*, vol. 72, no. 6, pp. 5426–5431, June 2024.

[14] X. Wang, S.-X. Gong, J. Ma, and C.-F. Wang, "Efficient analysis of antennas mounted on large-scale complex platforms using hybrid AIM-PO technique," *IEEE Trans. Antennas Propag.*, vol. 62, no. 3, pp. 1517–1523, Mar. 2014.

[15] X. Wang, H. X. Gong, S. Zhang, Y. Liu, R. P. Yang, and C. H. Liu, "Efficient RCS computation over a broad frequency band using subdomain MoM and Chebyshev approximation technique," *IEEE Access*, vol. 8, pp. 33522–33531, 2020.

[16] M. A. M. Hassan and A. A. Kishk, "A combined asymptotic waveform evaluation and random auxiliary sources method for wideband solutions of general-purpose EM problems," *IEEE Trans. Antennas Propag.*, vol. 67, no. 6, pp. 4010–4021, June 2019.

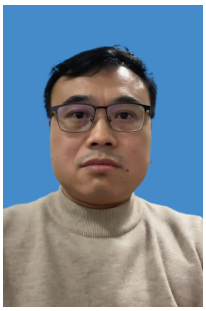

Junjun Wu was born in Shaanxi province, is a senior engineer at China Flight Test Research Institute and Xi'an Yuanfang Aviation Technology Development Co. Ltd. and is a master's candidate. His research direction is airborne antenna and their layout, including communication antenna, navigation antenna, beacon antenna as well as research on corresponding testing methods.